Algorithm Design For 3GPP NR Downlink Cell Search

Rahul Koduru, Rohit Budhiraja
Dept. of Electrical Engineering IIT Kanpur, Kanpur, India
{kpmrahul, rohitbr,}@iitk.ac.in

***Abstract*—Millimeter wave (mmWave) frequencies are being used for the 5th Generation(5G) cellular networks. We expect to have faster and highly reliable initial access procedures for NR. High directionality requirements at mmWave frequencies might affect the performance of initial access. We consider the beam acquisition configurations proposed for NR and propose two novel algorithms for beam detection and frame boundary acquisition for downlink cell search. We show that there is a trade off between the signalling overhead and detection reliability for different beam acquisition configurations.**

***Index Terms*—Initial Access (IA), new radio (NR), mmWave**

I. Introduction

Due to increasing demand for higher user data rates, and to serve increasing number of users, there is a need to enhance the current cellular networks. The 5th generation of cellular networks have recently been standardized by 3GPP in Release 15 as New Radio (NR), and are currently being developed. Use cases of NR include enhanced mobile broadband, ultra reliable low latency and Massive Machine communications. The mmWave spectrum provides larger bandwidths than the sub 6 GHz spectrum and enables large antenna arrays to be compactly placed at both base station and terminals [1].

Any terminal when it either switches on or enters a new cell, it needs to connect with a base station (BS). Initial access (IA) is the process which connects the terminal to a BS. IA includes cell search (CS) in the downlink and random access in the uplink [2]. The BS facilitates CS by periodically transmitting minimum system information through master information blocks (MIB). The terminal uses this information to estimate frame boundary, carrier frequency offset, and calculate cell ID which completes CS. Random access includes a series of message transfers between the BS and the terminal, after which a dedicated link is setup for information transmission. [3]

The existing literature has not yet investigated IA specifically for mmWave NR network except for a few recent studies in [2], [4]–[6]. Reference [2] evaluated IA performance through various beam sweeping configurations but it does not discuss beam selection procedures. Reference [4] evaluated beam management schemes proposed for initial access NR frameworks. However, the sparsity of synchronization signals across frequency domain in NR [7] is not considered in this work. References [5], [6] discussed a directional/omni beam generation scheme and exhaustive, iterative beam search procedures. This work, however did not provide any algorithm for beam selection. Also, reference [5] generates omni directional beam using a subset of available antennas, which will reduce the transmit power. Further, none of the aforementioned algorithms provided frame boundary acquisition.

The **main** contributions of this work help in bridging these gaps and can be summarized below.

- We propose a correlation-based and a generalized likelihood ratio test (GLRT)-based beam detection algorithms in initial access for NR mmWave systems.
- We propose novel frame-boundary acquisition through beam detection for NR mmWave systems. We note that none of the aforementioned references [2], [4]–[6] address the frame-boundary acquisition problem.
- The method proposed herein reduces the signalling overhead than the exhaustive search methods in [5]. We achieve this by considering NR-specific beam acquisition configurations. The proposed procedure employs a combination of narrow and broad omni-directional beams, *which are generated using all available antennas*.

The current work, to the best of our knowledge, is the first work which comprehensively addresses the downlink CS for NR mmWave systems.

II. Initial Access in NR

Initial Access in NR for mmWave frequencies is challenging as the MIB data signal cannot be transmitted omni-directionally due to shadowing and path loss [4], [6]. The BS should transmit MIB data signal directionally to combat shadowing and path loss. Further, angular directional beams should span a given region. For beam acquisition at the terminal and the BS, we briefly discuss a series of beam configurations [8],

- P1 - The BS covers a wide angular region using multiple broad beams while the terminal uses a single broad beam. The terminal selects a broader beam and reports it to the base station.
- P2 - The BS generates few narrow beams around the selected broader beam from P1 while the terminal uses a single broad beam. Through P2 a narrower beam gets selected.
- P3 - The BS uses the selected narrow beam in P2 while the terminal generates few narrow beams. The terminal decides the best narrow beam to be used.

The total number of beams required in this configuration is less compared to the beam configurations used in [5],

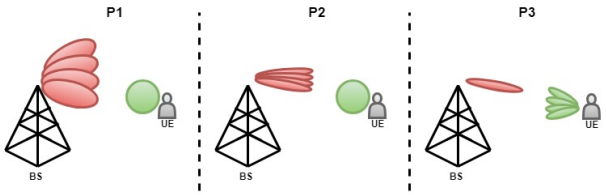

Fig. 1: Beam Acquisition Configurations.

[6]. Therefore, the above configuration reduces the required number of beams, reducing signalling overhead and also provides beam refinement at the BS.

III. Generation of Weight Vectors for Beam Antenna Configurations

We consider a mmWave NR BS and a NR terminal, which are equipped with $N_x \times N_y$ and $M_x \times M_y$ uniform planar array (UPA), respectively. Both BS and terminal use a full-analog antenna array architecture [1]. The beamforming vector used by the BS and the terminal are denoted as $\boldsymbol{w}_t$ and $\boldsymbol{w}_r$, respectively. The channel between them is modeled using 3GPP clustered delay line (CDL) models [9]. We next discuss the narrow beam and broad beam generation schemes for UPA which are used in P1, P2 and P3 steps.

A. Narrow beam generation

The beamforming vector to design beam for a UPA is given as [5]

$$\boldsymbol{w}_{upa}(\beta_x, \beta_y, N_x, N_y) = \boldsymbol{w}(\beta_x, N_x) \otimes \boldsymbol{w}(\beta_y, N_y), \quad (1)$$

where the vector $\boldsymbol{w}(\beta, N) = \frac{1}{\sqrt{N}}\left[1, \mathrm{e}^{-j\beta}, \cdots, \mathrm{e}^{-j(N-1)\beta}\right]^T$ with $\beta(\lambda, \theta, d) = \frac{2\pi d sin(\theta)}{\lambda}$ with $d \in \{d_x, d_y\}$, $\beta_x = \beta(\lambda, \theta, d_x)$ and $\beta_y = \beta(\lambda, \theta, d_y)$. Here $\otimes$ denotes kronecker product of the two vectors, the term d_x (resp. d_y) denotes the distance between each of the N_x (resp. N_y) antennas along x (resp. y) UPA direction. The term λ denotes the wavelength for the frequency of operation. The scalar θ denotes the azimuthal steering angle.

B. Broad Beam Generation

The terminal needs to generate omni-directional broad beam, with equal gains in all the azimuthal directions for the P1 and P2 steps. The broad beam generation problem can be modeled as

$$\mathbf{P1}: \text{find } \boldsymbol{w}$$
$$\text{s.t. } \boldsymbol{w}^H \boldsymbol{a}(\theta)\boldsymbol{a}(\theta)^H \boldsymbol{w} = 1, \forall\, \theta \in [0, \pi]$$
$$\text{and } \boldsymbol{w}^H \boldsymbol{w} = 1.$$

Here $\boldsymbol{w}$ is the beamforming vector used and $\boldsymbol{a}(\theta)$ is the array steering vector given as $\boldsymbol{a}(\theta) = \left[1, \mathrm{e}^{j\beta}, \cdots, \mathrm{e}^{j(N-1)\beta}\right]^T$, where $\beta = \frac{2\pi d sin(\theta)}{\lambda}$ is defined in the previous subsection. Reference [10] showed that $\mathbf{P1}$ does not have a solution unless we use only one antenna to generate the beam. A massive MIMO mmWave system radiates low power from each antenna. Using only one antenna of a massive MIMO system to generate broad beam will consequently not generate sufficient transmit power to combat fading at mmWave frequencies. Since we cannot create a perfect broad beam, we allow the beam to have very small deviations from the unity gain in different directions to generate a broad beam. We, therefore, introduce an error function in the first constraint. The updated broad beam generation problem is

$$\mathbf{P2}: \text{find } \boldsymbol{w}$$
$$\text{s.t. } \boldsymbol{w}^H \boldsymbol{a}(\theta)\boldsymbol{a}(\theta)^H \boldsymbol{w} = 1 + \varepsilon(\theta), \forall\, \theta \in [0, \pi]$$
$$\text{and } \boldsymbol{w}^H \boldsymbol{w} = 1.$$

Here $\varepsilon(\theta)$ is the error function introduced to the beam pattern which is a bounded function i.e, $|\varepsilon(\theta)| \leq \zeta$, for any scalar $\zeta \ll 1$. The solution of $\mathbf{P2}$ generates a broad beam with some deviations from unity gain [10]. This beam is generated from all the antennas, and therefore the generated signal has sufficient power to withstand fading at mmWave frequencies.

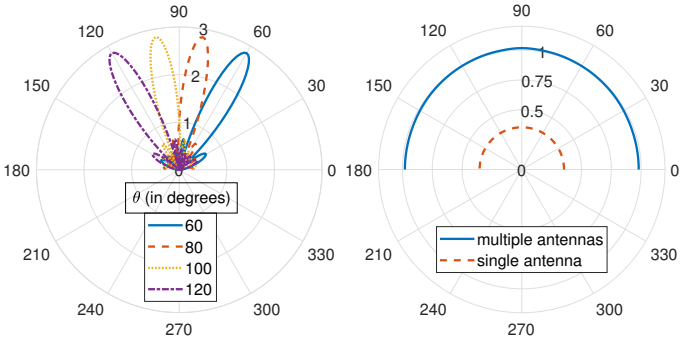

(a) Narrow beam pattern (b) Broad beam pattern

Fig. 2: Beam Patterns

Fig. 2a and Fig. 2b show the beam patterns for the narrow beams and broad beams for a 8x8 UPA antennas respectively. We see that narrow beams have different gains in different angular directions, and broad beams have almost equal gain for all angular directions and broad beam generated using multiple antennas has high transmit power.

IV. Cell Search Procedures

Before we discuss the CS procedure, we need to define a synchronizing signal (SS) block, which the BS transmits using a beam and the terminal receives using another beam.

A. SS block

A SS Block contains synchronization signals and MIB data required by the terminal to complete CS [3]. The NR defines two types of synchronization signals - primary synchronization signals (PSS) and secondary synchronization signals (SSS). The NR has 3 different PSS sequences (η_2) and 336 different SSS sequences (η_1) which together determine the cell ID(η), as follows $\eta = 3\eta_1 + \eta_2, \eta_2 \in \{0, 1, 2\}, \eta_1 \in \{0, 1, 2, \ldots, 335\}$. To calculate the cell ID, a terminal obtains the values of η_1 and η_2 by PSS and SSS sequence identification in the SS block. The SS block, along with the MIB, SSS and PSS, contains demodulation reference signals (DMRS) which are required by the terminal for channel estimation. The MIB data generated

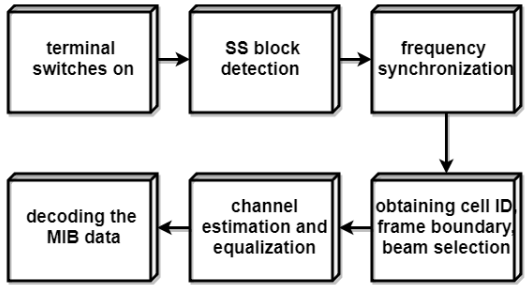

Fig. 3: Sequence of procedures at the terminal to complete CS.

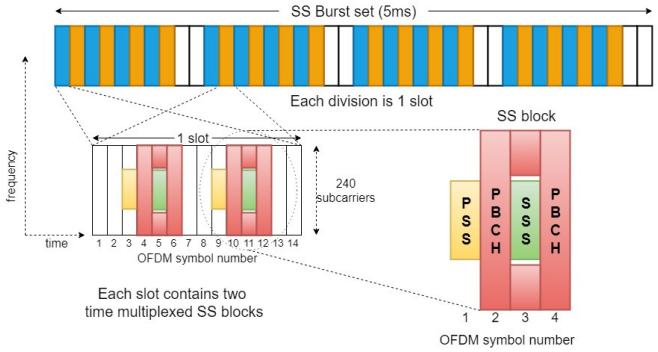

Fig. 4: SS burst set for a subcarrier spacing of 120 KHz

at higher layers is passed through a chain of physical layer procedures and mapped onto the SS block. The SS block has to be equalized and decoded at the terminal to obtain the MIB data which completes CS. Fig. 3 summarizes the sequence of procedures at the terminal to complete CS.

B. SS Burst set

Since the BS transmits a SS block using a beam, a given angular region is covered by transmitting SS blocks in a group which is repeated periodically with period between 5 ms to 80 ms, and is called a SS Burst set. The SS Burst set is defined to ensure that any terminal in the cell area receives a SS block without waiting for more than one SS Burst set time period [3]. For IA, a terminal assumes a periodicity of 20 ms. The total number of SS blocks in a set depends on the SS burst set configurations, which are defined for different subcarrier spacings [11]. Fig. 4 shows the structure of the SS Burst set for a subcarrier spacing of 120 kHz. Each division in the SS Burst set corresponds to a slot. All the coloured slots contain two time multiplexed SS blocks whose OFDM grid structure is shown.

V. SS Block Detection Algorithms

We now propose two different algorithms to select beam and estimate frame boundary through SS block detection. A terminal searches for SS block in the time domain, and we assume that it knows the carrier on which the SS Burst set is transmitted, and consequently does not perform carrier frequency search.

A. System model

For the analog antenna array architecture, the transmit signal vector is given as $\boldsymbol{x}[m] = \sqrt{P}\boldsymbol{w}_t s[m] = [x_1[m], x_2[m], \cdots, x_N[m]]^T$, where m is the time sample, P is the base station transmit power, $s[m]$ is the time domain signal generated at the base station, and $\boldsymbol{w}_t \in \mathbb{C}^{N\times 1}$ is the transmit beamforming vector with $N = N_x N_y$. The signal received by the terminal vector is given as $\boldsymbol{y}[m] = [y_1[m], y_2[m], \cdots, y_M[m]]^T$, where

$$y_j[m] = \sum_{i=1}^{N} h_{ij}[m] \circledast x_i[m] + n_j[m], \forall j \in \{1, 2, \ldots, M\}.$$

Here $M = M_x M_y$, the scalar $h_{ij}[m]$ denotes the channel impulse response between ith transmit and jth receive antenna, $n_j[m]$ are i.i.d. samples from a zero mean complex gaussian distribution with variance σ^2 i.e., $n_j[m] \sim C\mathcal{N}(0, \sigma^2)$. The signal at the receiver is combined using the receiver beamforming vector $\boldsymbol{w}_r \in \mathbb{C}^{M\times 1}$ as follows

$$\begin{aligned} r[m] &= \boldsymbol{w}_r^T \boldsymbol{y}[m] \\ &= \sum_{j=1}^{M} w_r(j) y_j[m] \\ &= \sum_{j=1}^{M} w_r(j) \left(\sum_{i=1}^{N} h_{ij}[m] \circledast x_i[m] + n_j[m] \right) \\ &= \sum_{j=1}^{M} w_r(j) \left(\sum_{i=1}^{N} h_{ij}[m] \circledast w_t(i) s[m] \right) + \underbrace{\sum_{j=1}^{M} w_r(i) n_j[m]}_{\tilde{n}[m]} \\ &= \underbrace{\left(\sum_{j=1}^{M} \sum_{i=1}^{N} w_r(j) w_t(i) h_{ij}[m] \right)}_{\tilde{h}[m]} \circledast s[m] + \tilde{n}[m] \\ &\triangleq \tilde{h}[m] \circledast s[m] + \tilde{n}[m]. \end{aligned} \tag{4}$$

Here the equivalent noise samples $\tilde{n}[m]$ are also i.i.d $C\mathcal{N}(0, \sigma^2)$. The received signal $r[m]$ is processed to accomplish cell search in the downlink.

B. Time domain PSS based correlation for SS block detection

We now exploit the low cross-correlation property of the PSS sequences, which are based on m-sequences [3], to propose a novel time domain beam detection algorithm. Since the positions of PSS symbols in the SS block are pre-stored in a terminal's memory, it consequently knows the time domain PSS signal generated by the base station. To estimate the location of time domain PSS signal in the received signal, a terminal correlates it with the pre-generated time domain PSS signals corresponding to the three η_2 values defined in Sect. IV. The cross correlation is given as

$$R_{rs_i}[l] = \sum_{k=-\infty}^{\infty} s_i^*[k] r[k+l] \,, \forall\, i = 0, 1, 2. \tag{5}$$

The term $s_i[k]$ denotes the kth sample of the pre-generated PSS time domain signal corresponding to $\eta_2 = i$ at the terminal, the term $r[k]$ denotes the kth sample of the received

time domain signal, scalar l denotes the delay between the two correlating signals. Now

$$\begin{aligned} R_{rs_i}[l] &= \sum_{k=-\infty}^{\infty} s_i^*[k]\left(\tilde{h}[k+l] \circledast x[k+l] + \tilde{n}[k+l]\right) \\ &= \sum_{k=-\infty}^{\infty} s_i^*[k]\Bigg(\sum_{\tau=-\infty}^{\infty} \tilde{h}[\tau]x[k+l-\tau] + \tilde{n}[k+l]\Bigg) \\ &= \sum_{\tau=-\infty}^{\infty} \tilde{h}[\tau]\Bigg(\underbrace{\sum_{k=-\infty}^{\infty} s_i^*[k]x[k+l-\tau]}_{R_{xs_i}[l-\tau]}\Bigg) + R_{\tilde{n}s_i} \\ &\triangleq \tilde{h}[l] \circledast R_{xs_i}[l] + R_{\tilde{n}s_i}. \end{aligned} \tag{6}$$

Here R_{xs_i} and $R_{\tilde{n}s_i} = \sum_{k=-\infty}^{\infty} s_i[k]^*\tilde{n}[k+l]$ denotes the cross correlation function of the transmit signal $x[m]$, noise $\tilde{n}[m]$ with the reference signal $s_i[m]$ respectively. The problem to detect the strongest beam with the SS block can be posed as

$$(i_0, l_0) = \underset{i,\, l}{\arg\max}\ R_{rs_i}[l]. \tag{7}$$

Here the i_0, and the l_0 denote the PSS sequence, and the delay at which the highest correlation peak is observed. The two factors which result in the peak, which can be seen from (6) are low cross correlation property of PSS sequences included in $R_{xs_i}[l]$, and the alignment of transmit/receive beams along the strongest channel direction implicitly included in $\tilde{h}[l]$.

C. Time domain GLRT for SS block detection

Generalized Likelihood Ratio Test (GLRT) poses the SS block detection problem as a hypothesis testing problem. We define two hypotheses, Ω_1 and Ω_2, corresponding to the presence or absence of the PSS time domain sequence of length F, FFT size. The log ratio of the likelihoods of the hypotheses gives us a measure to confirm a hypothesis. For the system model defined in (4), the length F samples vector of received signal for the hypotheses can be modeled as

$$\Omega_1 : \boldsymbol{r}_1[l] = \boldsymbol{\mu_i} + \boldsymbol{n}[l] \quad \text{(PSS sequence present)},$$
$$\Omega_2 : \boldsymbol{r}_2[l] = \boldsymbol{n}[l] \quad \text{(PSS sequence absent)}.$$

Here the scalar l denotes a given time sample, the vector $\boldsymbol{\mu}_i = [\mu_i[0], \mu_i[1], \cdots, \mu_i[F-1]]^T\ \forall\ i = \{0, 1, 2\}$ denotes the presence of the signal component and can be obtained by $\mu_i[k] = \tilde{h}[k] \circledast s_i[k]\ \forall\ k = \{0, 1, \ldots, F-1\}$, ,the noise vector $\boldsymbol{n}[l] = \begin{bmatrix}\tilde{n}[l] & \tilde{n}[l+1] & \ldots & \tilde{n}[l+F-1]\end{bmatrix}^T$, the scalars $\tilde{h}[m]$ and $\tilde{n}[m]$ are defined in (4), $s_i[k]$ is defined in (5). The likelihood probabilities of the two hypotheses are given as

$$\begin{aligned} p\left(\boldsymbol{r_g}[l] \,\middle|\, \tilde{h}, \Omega_1\right) &= k\exp\left(-\frac{1}{2}(\boldsymbol{r_g}[l] - \boldsymbol{\mu}_i)^H\boldsymbol{\Sigma}^{-1}(\boldsymbol{r_g}[l] - \boldsymbol{\mu}_i)\right) \\ p\left(\boldsymbol{r_g}[l] \,|\, \Omega_2\right) &= k\exp\left(-\frac{1}{2}\boldsymbol{r_g}[l]^H\boldsymbol{\Sigma}^{-1}\boldsymbol{r_g}[l]\right). \end{aligned} \tag{8}$$

Here the scalar $k = \left((2\pi)^F \mid \boldsymbol{\Sigma} \mid\right)^{-1}$, the vector $\boldsymbol{r_g}[l] = [r[l], r[l+1], \cdots, r[l+F-1]]^T$ consists of F consecutive time samples of the received signal at the terminal starting from the lth sample, $\boldsymbol{\Sigma}$ denotes the correlation matrix of $\boldsymbol{n}[l]$, given as $\boldsymbol{\Sigma} = \sigma^2\boldsymbol{I}_F$. As the channel is unknown, $\boldsymbol{\mu}_i$ is also unknown to the terminal. We use the maximum likelihood channel estimate to calculate $\boldsymbol{\mu}_i$. The channel is assumed to be a L tap channel, the taps are given by $\tilde{h}[0], \tilde{h}[1], \cdots, \tilde{h}[L-1]$. The vector $\boldsymbol{\mu}_i$ can further be expressed as

$$\boldsymbol{\mu}_i = \boldsymbol{S}\boldsymbol{h}_{tap}, \text{ where}$$

$$\boldsymbol{h}_{tap} = \begin{bmatrix}\tilde{h}[0] & \tilde{h}[1] & \ldots & \tilde{h}[L-1]\end{bmatrix}^T$$

$$\boldsymbol{S} = \begin{bmatrix} s_i[0] & s_i[F-1] & \ldots & s_i[F-L+1] \\ s_i[1] & s_i[0] & \ldots & s_i[F-L+2] \\ \vdots & \vdots & \ddots & \vdots \\ s_i[F-1] & s_i[F-2] & \ldots & s_i[F-L] \end{bmatrix}.$$

The $\boldsymbol{\mu}_i$ is calculated by maximizing $p\left(\boldsymbol{r_g}[l] \,\middle|\, \tilde{h}, \Omega_1\right)$ with respect to the parameter $\boldsymbol{h}_{tap}$ as follows

$$\begin{aligned} \hat{\boldsymbol{h}}_{tap} = \underset{\boldsymbol{h}_{tap}}{\arg\max}\ p\left(\boldsymbol{r_g}[l] \,\middle|\, \tilde{h}, \Omega_1\right) &\equiv \underset{\boldsymbol{h}_{tap}}{\arg\min}\ \|\boldsymbol{r_g}[l] - \boldsymbol{\mu}_i\|^2 \\ &\equiv \underset{\boldsymbol{h}_{tap}}{\arg\min}\ \|\boldsymbol{r_g}[l] - \boldsymbol{S}\boldsymbol{h}_{tap}\|^2 \\ &= (\boldsymbol{S}^H\boldsymbol{S})^{-1}\boldsymbol{S}^H\hat{\boldsymbol{r}}[l] \\ \Rightarrow \boldsymbol{\mu}_i &= \boldsymbol{S}\hat{\boldsymbol{h}}_{tap}. \end{aligned} \tag{9}$$

Now that we have obtained $\boldsymbol{\mu}_i$, the log likelihood ratio (LLR) is given as

$$\begin{aligned} \text{LLR} &= \ln\left(\frac{p\left(\boldsymbol{r_g}[l] \,\middle|\, \tilde{h}, \Omega_1\right)}{p\left(\boldsymbol{r_g}[l] \,|\, \Omega_2\right)}\right) \\ &= \ln\left(\frac{k\exp\left(-\frac{1}{2}(\boldsymbol{r_g}[l] - \boldsymbol{\mu}_i)^H\boldsymbol{\Sigma}^{-1}(\boldsymbol{r_g}[l] - \boldsymbol{\mu}_i)\right)}{k\exp\left(-\frac{1}{2}\boldsymbol{r_g}[l]^H\boldsymbol{\Sigma}^{-1}\boldsymbol{r_g}[l]\right)}\right) \\ &= \ln\left(\frac{\exp\left(-\frac{\|\boldsymbol{r_g}(l) - \boldsymbol{\mu}_i\|^2}{2\sigma^2}\right)}{\exp\left(-\frac{\|\boldsymbol{r_g}(l)\|^2}{2\sigma_t^2}\right)}\right) \\ &= \frac{1}{2\sigma^2}(\|\boldsymbol{r_g}(l)\|^2 - \|\boldsymbol{r_g}(l) - \boldsymbol{\mu}_i\|^2). \end{aligned} \tag{10}$$

Now that the measure is derived, the strongest SS block detection problem which helps to select a beam is posed as,

$$(i_0, l_0) = \underset{i,\, l}{\arg\max}\ \text{LLR}. \tag{11}$$

Here i_0 and l_0 denote the PSS sequence index and the delay at which the highest correlation peak is observed.

D. Beam selection and frame boundary acquisition

The above two algorithms yield the PSS sequence index i_0, and the delay at which the highest peak is observed l_0 in (7) and (11),. Here i_0 gives us the value of η_2, and l_0 denotes the start of PSS time domain sequence of the strongest SS block in the received signal. The SS blocks contain information about its location in the SS burst set, which is known as the SS block index (i_{ssb}) and can be obtained at the terminal by the DMRS sequence identification and MIB decoding [11]. This i_{ssb} is fed back to the base station which obtains the beam associated with that SS block for P1, and P2 steps. For the P3 step, the beam is obtained directly as the terminal knows the beam associated with the SS block. Let l_s denote the time domain samples from the start of the SS burst set to the SS

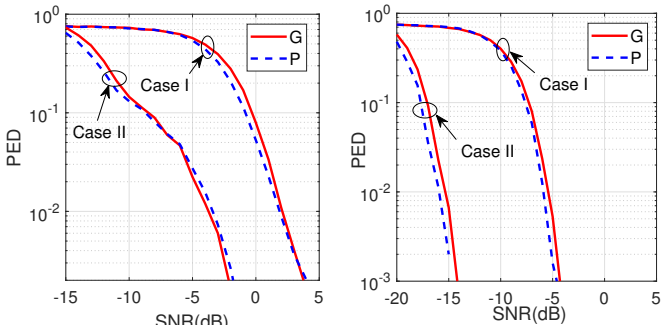

(a) CDL-A (b) CDL-D

Fig. 5: PED versus SNR for a) CDL-A and b) CDL-D models

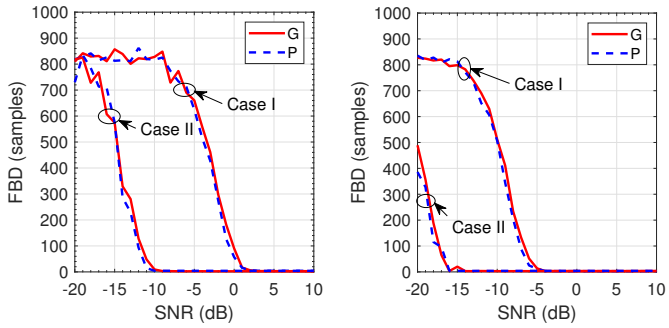

(a) CDL-A (b) CDL-D

Fig. 6: FBD versus SNR for a) CDL-A and b) CDL-D models

block given by i_{ssb}. The sample at which the frame boundary is present at the terminal is given by "$l_0 - l_s$".

VI. Simulation Results

We now numerically evaluate the performance of the two proposed SS block detection algorithms given by (7) and (11) based on probability of error detection (PED) of the strongest SS block and frame boundary deviation (FBD) of the frame boundary obtained from the actual. We chose PED and FBD as metrics for detection reliability. For this study we consider a system $N_x = N_y = 8$, $M_x = M_y = 4$ which is operating at 28 GHz. The bandwidth allocated for the SS Burst set transmission is 25 resource blocks with a subcarrier spacing of 120 kHz. We plot for PED and FBD versus SNR, where SNR = P/σ^2. We consider two beam configurations for SS block detection -

- Case I : Narrow beams are used at the BS and a single broad beam is used at the terminal.
- Case II : Narrow beams are used at the BS and the terminal.

Case I denotes the P1 configuration of Fig. 1 and is used to compare the performance of the proposed configurations for beam acquisition in sect. II with the configurations of [5], [6] denoted by Case II.

Fig. 5 shows PED versus SNR plots for the SS block detection algorithms for CDL-A and CDL-D channel models [9]. G and P in the figures denote GLRT and PSS correlation methods respectively. Similarly, Fig. 6 shows FBD versus SNR plots. We can see that PED and FBD values are similar for the two proposed algorithms for similar beam configuration and channel model. For SNR > 5 dB, the PED values are almost negligible and FBD reduces to zero. We observe at low SNR regime, case I has degraded performance than case II but case I is required by P1/P2/P3 configurations to reduce signalling overhead as explained in sect. II. There is, therefore, a trade off between the signalling overhead, and the reliability for SS block detection while using different beam acquisition configurations.

Summary: For high SNR values, we can use the P1/P2/P3 configurations, which reduces the signalling overhead with a reliable detection. For low SNR value, it is better to use exhaustive search using narrow beams at base station and terminal to obtain the beam pair even though signalling overhead increases.

VII. Conclusions

We proposed two novel algorithms for beam detection and frame boundary acquisition for cell search in NR. We numerically investigated the performances of these algorithms for different beam configurations specified in the NR. We suggested, for different SNR regimes, the beam pair detection method and the beam acquisition configuration to be used.

References

[1] R. W. Heath, N. González-Prelcic, S. Rangan, W. Roh, and A. M. Sayeed, "An overview of signal processing techniques for millimeter wave mimo systems," *IEEE J. Sel. Topics Signal Process.*, vol. 10, no. 3, pp. 436–453, April 2016.

[2] Y. Li, J. G. Andrews, F. Baccelli, T. D. Novlan, and C. J. Zhang, "Design and analysis of initial access in millimeter wave cellular networks," *IEEE Trans. Wireless Commun.*, vol. 16, no. 10, pp. 6409–6425, Oct 2017.

[3] E. Dahlman, S. Parkvall, and J. Skold, *5G NR: The Next Generation Wireless Access Technology*. Elsevier Science, 2018. [Online]. Available: https://books.google.co.in/books?id=lcSLswEACAAJ

[4] M. Giordani, M. Polese, A. Roy, D. Castor, and M. Zorzi, "Initial access frameworks for 3gpp nr at mmwave frequencies," in *2018 17th Annual Mediterranean Ad Hoc Networking Workshop (Med-Hoc-Net)*, June 2018, pp. 1–8.

[5] L. Wei, Q. C. Li, and G. Wu, "Initial access techniques for 5g nr: Omni/beam sync and rach designs," in *2018 International Conference on Computing, Networking and Communications (ICNC)*, March 2018, pp. 249–253.

[6] M. Giordani, M. Mezzavilla, C. N. Barati, S. Rangan, and M. Zorzi, "Comparative analysis of initial access techniques in 5g mmwave cellular networks," in *2016 Annual Conference on Information Science and Systems (CISS)*, March 2016, pp. 268–273.

[7] 3GPP, "NR; Base Station (BS) radio transmission and reception," 3rd Generation Partnership Project (3GPP), Technical Specification (TS) 38.104, 01 2018, version 15.0.0. [Online]. Available: http://www.3gpp.org/DynaReport/38104.htm

[8] 3GPP, "Study on new radio access technology Physical layer aspects," 3rd Generation Partnership Project (3GPP), Technical Report (TR) 38.802, 09 2017, version 14.2.0. [Online]. Available: http://www.3gpp.org/DynaReport/38802.htm

[9] 3GPP, "Study on channel model for frequencies from 0.5 to 100 GHz," 3rd Generation Partnership Project (3GPP), Technical Report (TR) 38.901, 01 2018, version 14.3.0. [Online]. Available: http://www.3gpp.org/DynaReport/38901.htm

[10] D. Qiao, H. Qian, and G. Y. Li, "Broadbeam for massive mimo systems," *IEEE Trans. Signal Process.*, vol. 64, no. 9, pp. 2365–2374, May 2016.

[11] 3GPP, "NR; Physical layer procedures for control," 3rd Generation Partnership Project (3GPP), Technical Specification (TS) 38.213, 01 2018, version 15.0.0. [Online]. Available: http://www.3gpp.org/-DynaReport/38213.htm